



**CHALMERS**  
UNIVERSITY OF TECHNOLOGY

## **Graphite paper / carbon nanotube composite: A potential supercapacitor electrode for powering microsystem technology**

Downloaded from: <https://research.chalmers.se>, 2023-05-28 07:23 UTC

Citation for the original published paper (version of record):

Li, Q., Smith, A., Haque, M. et al (2017). Graphite paper / carbon nanotube composite: A potential supercapacitor electrode for powering microsystem technology. *Journal of Physics: Conference Series*, 922(1).  
<http://dx.doi.org/10.1088/1742-6596/922/1/012014>

N.B. When citing this work, cite the original published paper.

# Graphite paper / carbon nanotube composite: a potential supercapacitor electrode for powering microsystem technology

Qi Li, Anderson D. Smith, Mazharul Haque, Agin Vyas, Volodymyr Kuzmenko, Per Lundgren, Peter Enoksson

Chalmers University of Technology, Gothenburg, Sweden

qili@chalmers.se

**Abstract.** This work describes fabrication of a flexible supercapacitor electrode. The fabrication starts with graphite paper (GP). Carbon nanotubes (CNTs) are then grown directly to the carbon surface by chemical vapor deposition (CVD), forming a heterogeneous structure of GP/CNT. The integration of CNT enhances capacitive performance while maintaining the flexibility of GP, thus making GP/CNT a promising supercapacitor electrode material for potentially powering microsystem technology.

## 1. Introduction

Recent advances in MEMS allow nearly seamless integration of an array of actuators and/or sensors to multi-functionalize a device [1]. Benefiting from that, smart systems such as wearable electronics have attracted tremendous attention worldwide and a rapid development is ongoing in recent years to explore the potential of these technologies [2]. Unfortunately, many potential applications are limited by power management [3] and the lifetime of the energy storage component [4].

Supercapacitors, also known as ultracapacitors and electrochemical capacitors, have the ability to deliver near instantaneous energy, work with less complicated circuits and have almost limitless lifetime [5, 6]. These characteristics make this type of energy storage devices suitable for powering MEMS-based systems, especially for those with power consumption as low as microwatts. Additionally, since form factor is critical for wearable technology and many other miniaturized smart systems [1], flexibility of the supercapacitor is advantageous. The flexibility allows the possibility of rolling or folding up an energy storage device to achieve high space-efficiency.

In this paper, we present a fabrication of a flexible electrode material for supercapacitors. The fabrication begins with a sheet of graphite paper (GP) and then compositing with direct carbon nanotube (CNT) growth by chemical vapor deposition (CVD) in 10 seconds. The resulting GP/CNT material is flexible, shows high areal capacitance and cycling stability. Since the GP substrate has a good heat dissipation ability [7], the supercapacitors based on this GP/CNT composite is also possibly capable of carrying high working current without over-heating problems. Taken all into account, GP/CNT composite are potentially suitable for supercapacitors integrable to various advanced electronics.



## 2. Experimental

### 2.1. Fabrication of GP/CNT

The fabrication of GP/CNT consists of two primary steps: catalyst deposition onto the GP and subsequent CVD growth. First, 2 nm Fe and 3 nm Al<sub>2</sub>O<sub>3</sub> layer was deposited successively on the surface of graphite paper (GP) using e-beam evaporation. The arrangement of Fe under Al<sub>2</sub>O<sub>3</sub> layer is designed for tip growth of CNTs during CVD process. After catalyst deposition, the GP was placed on a graphite heater mounted in a glass chamber at a pressure below 0.1 mbar. A hydrogen flow of 837 sccm was then introduced into the chamber and the heater ramped up to 500 °C and maintained at this temperature for 3 min. Afterwards, the heater temperature is rapidly increased to 700 °C, while acetylene at a rate of 240 sccm was purged into the chamber for 10 seconds – resulting in vertical CNT growth of 1-2 μm in length.

### 2.2. Materials characterization

The morphology of GP and GP/CNT materials was examined by scanning electron microscopy (using a SEM, Zeiss Supra 60 VP). Raman spectra and spectra mapping were recorded using a Raman spectrometer (Horiba) with a 638 nm excitation laser.

### 2.3. Electrochemical measurements

A supercapacitor device (2032 coin cell) was assembled using GP/CNT composite as the electrodes for the initial demonstration of performance. Two identical electrode pellets with diameter of 14 mm were punched out of the corresponding films with a disc cutter. The electrodes were separated by a Whatman® glass fiber membrane of 16 mm diameter. The coin cell was then filled with 50 μl 6 M KOH electrolyte.

The electrochemical measurements were conducted with a Gamry Reference 3000AE at room temperature, 21 °C. The measurements included cyclic voltammetry (CV), galvanostatic charge/discharge (GCD) and cyclic charge/discharge (CCD).

The areal capacitance (mF cm<sup>-2</sup>) was calculated from GCD measurements using  $C = I_{\text{dis}} t_{\text{dis}} / V$ , where  $I_{\text{dis}}$  (mA cm<sup>-2</sup>) is the constant discharge areal current (area normalized to 1.5383 cm<sup>2</sup>),  $t_{\text{dis}}$  (s) is the discharge time, and  $V$  is the cell voltage excluding IR drop. The areal energy density  $E$  (μWh cm<sup>-2</sup>) and areal power density  $P$  (μW cm<sup>-2</sup>) were obtained by applying the following equations, respectively:  $E = 0.5 C V^2 / 3.6$ ,  $P = 3600 E / t_{\text{dis}}$ .

## 3. Results and discussion

### 3.1 Materials characterization

The surface morphology of GP and GP/CNT is shown in Figure 1. The GP material of grey colour has a relatively smooth surface (Figure 1a). In contrast, the surface becomes rougher since it is covered with CNT bundles (Figure 1b) after the catalyst deposition and CVD process, and the material appearance turns black. A typical structure of the CNT bundles is displayed in Figure 1c-d: CNTs of 1-2 μm attach directly to the carbon (graphite) substrate, while Fe and Al<sub>2</sub>O<sub>3</sub> residing at the CNT tips are lifted to the surface. Such a structure is a result of the specific definition of catalyst layers, i.e. Fe under Al<sub>2</sub>O<sub>3</sub>, which enables an tip growth of CNT [8]. The surface of GP/CNT is non-continuous (Figure 1b-c), because of cracking of the Al<sub>2</sub>O<sub>3</sub> layer in the presence of hydrogen gas at elevated temperature. It is worth noting that the graphite substrate has great flexibility (Figure 1e), and such a merit is inherited by the GP/CNT composite, making it interesting for flexible/wearable electronics. Additionally, direct attachment of CNTs to the carbon surface potentially facilitates fast electron transport and thus good supercapacitor performance [9] in terms of high power capability.

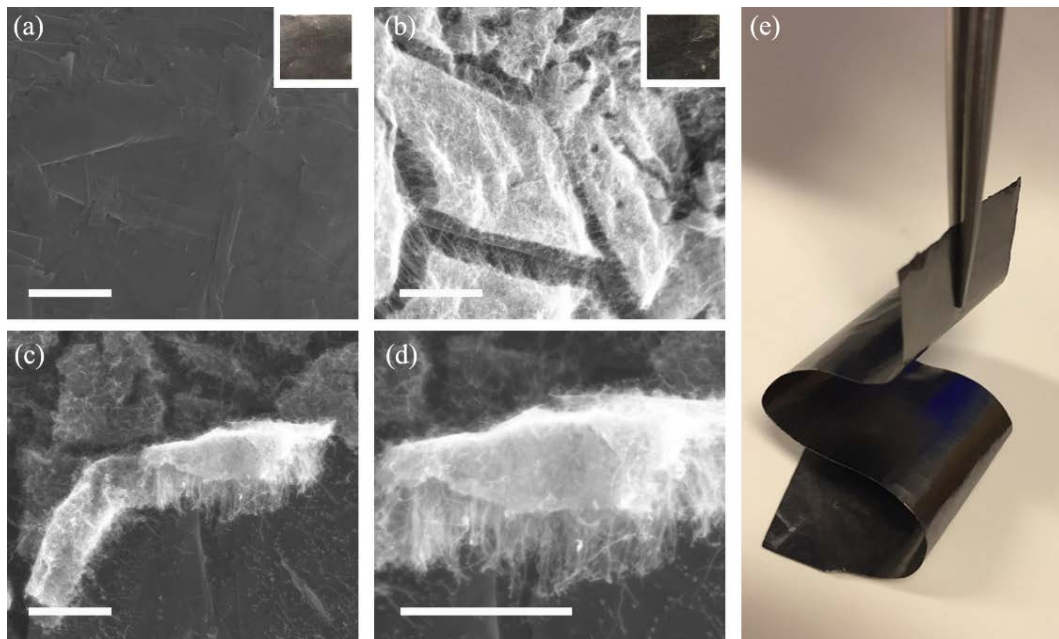


**Figure 1.** SEM images of (a) GP and (b-d) GP/CNT, and (e) demonstration of GP flexibility. The insets in (a-b) are the optical pictures of corresponding material. Scale bar in (a-d) is 1  $\mu\text{m}$ .

Raman spectra were recorded in order to confirm the successful growth of CNTs and examine the CNT quality. Figure 2a shows the spectra of GP substrate and GP/CNT composite. GP spectrum is characterized by typical graphite features, with D, G, 2D bands at approx. 1330, 1580 and 2750  $\text{cm}^{-1}$ , respectively. For GP/CNT, its G band clearly splits into  $G^+$  and  $G^-$ . The doublet G band peak is attributed to a slight carbon sheet curvature and is considered as signature of CNTs.

The G band is derived from the carbon lattice stretching of the  $\text{sp}^2$  bonded graphene plane, whereas the D band originates from the defect structure in the honeycomb graphene-like lattice [10]. The intensity ratio of G to D bands ( $I_G/I_D$ ) is correlated with the amount of defects in graphitic materials, and can be used to reflect the quality of CNTs [11]. A mapping image of  $I_G/I_D$  within a selected ca.  $20 \times 20 \mu\text{m}^2$  area is shown in Figure 2b. Representative spectra at the three specified spots are displayed in Figure 2c. The D,  $G^-$ ,  $G^+$  and  $G'$  band positions are identical for the three selected spots, with  $I_G/I_D$  ratio ranging from the lowest (5.7) to highest (7.7). Considering the non-continuous surface morphology (meaning that exposed graphite between cracks contributes to the G band signals), the Raman mapping data indicates a rather reasonable homogeneity of CNT quality.

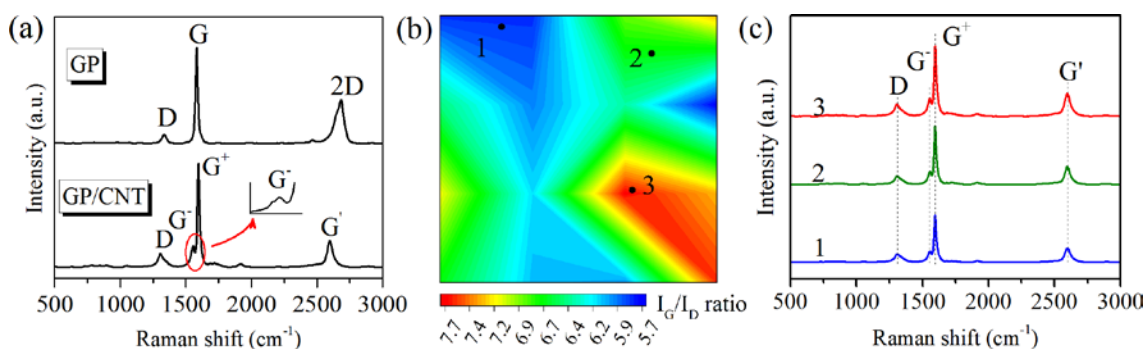


**Figure 2.** (a) Raman spectra of GP and GP/CNT, (b) Raman mapping of an approx.  $20 \times 20 \mu\text{m}^2$  area on GP/CNT, and (c) comparison of Raman spectra at the three specified spots in (b).

### 3.2. Device performance

As previously mentioned, the fabricated GP/CNTs were used as electrodes in a supercapacitor for performance assessment. The CV curves are shown in Figure 3a-g. At lower scan rates, the device displays rectangular CV characteristics, which are indicative of double layer capacitive mechanism (commonly observed for carbon-based materials). With an increasing scan rate, the response current increases, while the CV curve correspondingly deviates from rectangular to quasi-rectangular shape. The current response remains linear to scan rates up to  $1000 \text{ mV s}^{-1}$  (Figure 3h), and the responsive CV curve is still symmetric up to  $100000 \text{ mV s}^{-1}$  (i.e.  $100 \text{ V s}^{-1}$ ), indicating that the GP/CNT material has a good rate capability.

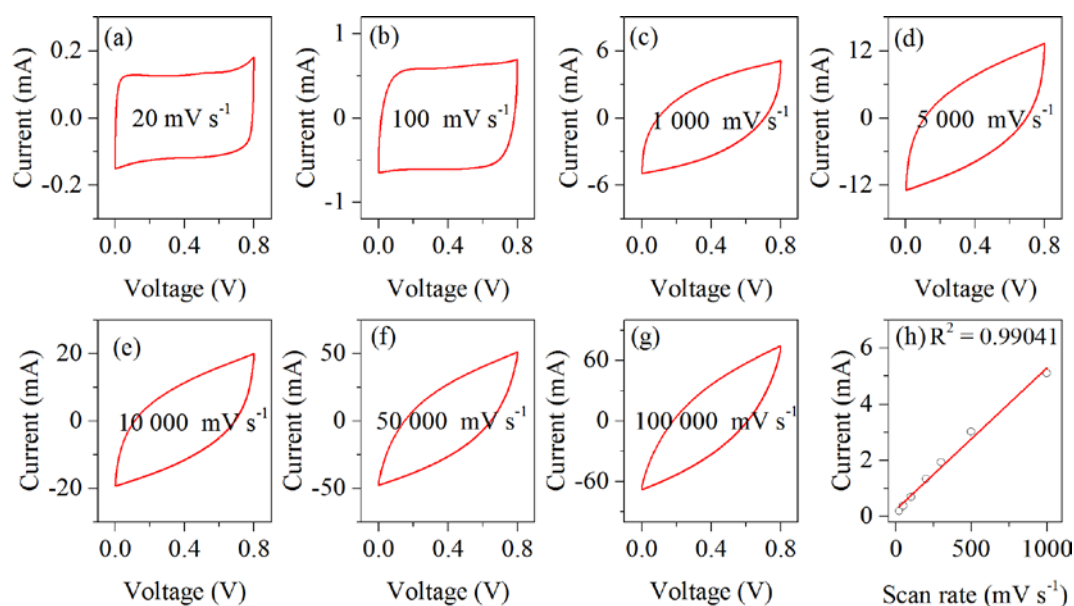


**Figure 3.** Cyclic voltammetry (CVs) of GP/CNT at specified scan rates (a-g), and (h) evolution of the cathodic current versus scan rate till  $1000 \text{ mV s}^{-1}$ .

GCD curves at different current densities are displayed in Figure 4a-b. In agreement with CV measurements, GP/CNT exhibits typical double layer GCD features of triangular curves. The highest areal capacitance of  $4.4 \text{ mF cm}^{-2}$  is achieved at the lowest current of  $0.1 \text{ mA cm}^{-2}$ . With the current density ramping up, the capacitance decreases to  $0.8 \text{ mF cm}^{-2}$  at a rather high current density of  $15 \text{ mA cm}^{-2}$  (Figure 4c). Accordingly, the maximum ( $0.38 \text{ } \mu\text{Wh cm}^{-2}$ ) and minimum ( $0.04 \text{ } \mu\text{Wh cm}^{-2}$ ) energy, and the minimum ( $29 \text{ } \mu\text{W cm}^{-2}$ ) and maximum ( $1790 \text{ } \mu\text{W cm}^{-2}$ ) power density are achieved at  $0.1$  and  $15 \text{ mA cm}^{-2}$ , respectively. It is worth noting that pure GP has much lower capacitance than GP/CNT as compared in Figure 4c, indicating that the energy of GP/CNT composite material mostly originates from the CVD grown CNTs.

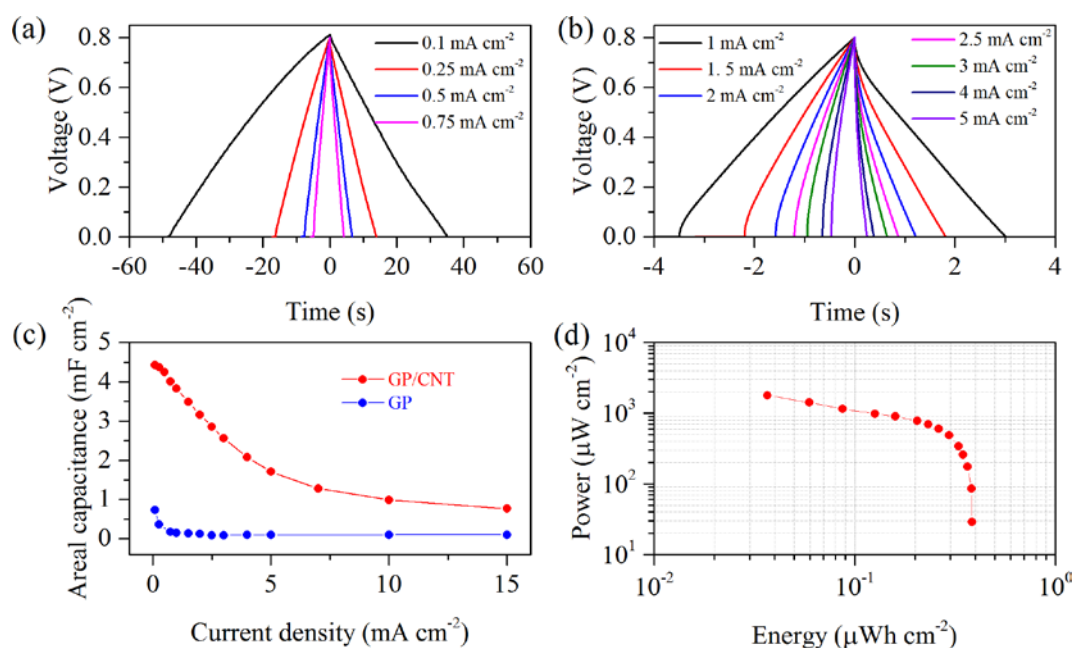


**Figure 4.** (a-b) Galvanostatic charge/discharge (GCD) curves of GP/CNT at different current densities; (c) The calculated areal capacitance of GP and GP/CNT at different current densities; (d) Ragone plot of GP/CNT.

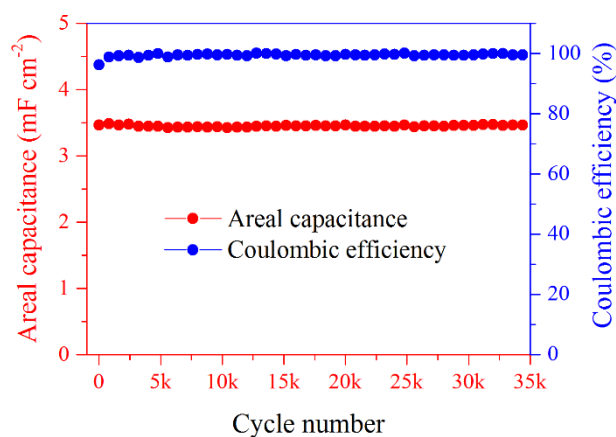


**Figure 5.** Cyclic charge/discharge (CCD) measurement at 2 mA cm<sup>-2</sup>.

The GP/CNT-based supercapacitor also shows very high stability. The charge/discharge measurements repeated up to 35000 cycles with no observed decrease in capacitance. The coulombic efficiency (the ratio of discharge capacity to charge capacity) is close to 100% throughout the whole process.

#### 4. Conclusions and future work

A freestanding flexible graphite paper composited with carbon nanotubes (GP/CNT) was successfully fabricated with the assistance of CVD-based CNT growth. The obtained GP/CNT material shows promising electrochemical performance as a supercapacitor electrode. The material flexibility makes the GP/CNT interesting as an energy storage component in flexible and wearable electronics as well as powering various microsystems. Future work can be directed into the following aspects: (1) Energy enhancement by increasing the CNT content or by compositing with pseudocapacitive materials; (2)



Rate capability improvement by removing the Fe/Al<sub>2</sub>O<sub>3</sub> layer; (3) Fabrication of all-solid-state flexible supercapacitors; (4) Integration of supercapacitor components with other microsystem technologies such as sensors, MEMS harvesters and digital electronics.

### Acknowledgements

This work was funded by the European Union's Horizon 2020 research and innovation program smart-MEMPHIS project (grant number 644378), and the Vinnova UDI project Energy Harvesting Toolkit.

### References

- [1] D. Heussner, Wearable Technologies Present Packaging Challenges, *Electronic Design*, (2014).
- [2] X. Tao, *Wearable electronics and photonics*, Elsevier, 2005.
- [3] Y. Zi, H. Guo, J. Wang, Z. Wen, S. Li, C. Hu, Z.L. Wang, An Inductor-Free Auto-Power-Management Design Built-in Triboelectric Nanogenerators, *Nano Energy*, 31 (2017) 302-310.
- [4] M. Magno, T. Polonelli, F. Casamassima, A. Gomez, E. Farella, L. Benini, Energy-Efficient Context Aware Power Management with Asynchronous Protocol for Body Sensor Network, *Mobile Networks and Applications*, (2016) 1-11.
- [5] Z. Fan, J. Yan, T. Wei, L. Zhi, G. Ning, T. Li, F. Wei, Asymmetric Supercapacitors Based on Graphene/MnO<sub>2</sub> and Activated Carbon Nanofiber Electrodes with High Power and Energy Density, *Advanced Functional Materials*, 21 (2011) 2366-2375.
- [6] Q. Li, M. Haque, V. Kuzmenko, N. Ramani, P. Lundgren, A.D. Smith, P. Enoksson, Redox Enhanced Energy Storage in an Aqueous High-Voltage Electrochemical Capacitor with a Potassium Bromide Electrolyte, *Journal of Power Sources*, 348 (2017) 219-228.
- [7] S. Jain, O. Yehia, L. Qiao, Flame Speed Enhancement of Solid Nitrocellulose Monopropellant Coupled with Graphite at Microscales, *Journal of Applied Physics*, 119 (2016) 094904.
- [8] C.L. Pint, N.T. Alvarez, R.H. Hauge, Odako Growth of Dense Arrays of Single-Walled Carbon Nanotubes Attached to Carbon Surfaces, *Nano Research*, 2 (2009) 526-534.
- [9] Y. Zhu, L. Li, C. Zhang, G. Casillas, Z. Sun, Z. Yan, G. Ruan, Z. Peng, A.-R.O. Raji, C. Kittrell, A Seamless Three-Dimensional Carbon Nanotube Graphene Hybrid Material, *Nature Communications*, 3 (2012) 1225.
- [10] N.G. Yasri, A.K. Sundramoorthy, W.-J. Chang, S. Gunasekaran, Highly Selective Mercury Detection at Partially Oxidized Graphene/Poly(3,4-Ethylenedioxythiophene):Poly(Styrenesulfonate) Nanocomposite Film-Modified Electrode, *Frontiers in Materials*, 1 (2014).
- [11] I.V. Anoshkin, I.I. Nefedova, D.V. Lioubtchenko, I.S. Nefedov, A.V. Räsänen, Single Walled Carbon Nanotube Quantification Method Employing the Raman Signal Intensity, *Carbon*, 116 (2017) 547-552.